


Image-enhanced bipolaron formation at organic semiconductor/electrode interfacesJonathon R. Schreengost,¹ Sukrit Mukhopadhyay,² and Noel C. Giebink^{3,*}¹*Department of Materials Science and Engineering, The Pennsylvania State University, University Park, Pennsylvania 16802, USA*²*The Dow Chemical Company, 1776 Building, Midland, Michigan 48674, USA*³*Department of Electrical Engineering, The Pennsylvania State University, University Park, Pennsylvania 16802, USA* (Received 8 July 2020; revised 21 September 2020; accepted 6 October 2020; published 21 October 2020)

We explore the image charge interaction for organic semiconductor bipolarons near a conducting interface and find that the cross term between one of the constituent charges and the image of its neighbor stabilizes the bipolaron by up to ~ 0.3 eV, dramatically increasing the concentration of this species near the interface. Using density functional theory calculations for the common hole transport molecule *N,N'*-bis(3-methylphenyl)-*N,N'*-diphenylbenzidine, we validate a simple point charge description of this effect and incorporate it within an interface energy level alignment model to predict the density of polarons and bipolarons near the interface. We find that the image effect greatly enhances bipolaron formation in the first few monolayers, leading to the expectation that bipolarons account for more than 1% of the total interface charge in many cases of practical interest. This result reinforces the notion that bipolarons are robust near the contacts of many organic semiconductor devices and thus helps to rationalize their involvement in the phenomenon of unipolar organic magnetoresistance.

DOI: [10.1103/PhysRevB.102.165311](https://doi.org/10.1103/PhysRevB.102.165311)**I. INTRODUCTION**

Strong Coulomb repulsion between like-signed charge carriers in organic semiconductors typically prevents two electrons or two holes from occupying a single molecule or conjugated polymer segment. The quasiparticle that results from such an event—a bipolaron—is partially stabilized by relaxation of the nuclear framework and polarization of the surroundings, resulting in a net energy barrier for bipolaron formation, U_0 , known as the Hubbard energy [1]. Although U_0 is generally large compared to the thermal energy ($U_0 > 0.1$ eV), strong energetic disorder in organic thin films can compensate to some extent (i.e., by hopping from a higher- to a lower-energy molecular site), resulting in non-negligible bipolaron densities that may explain phenomena such as unipolar organic magnetoresistance [2].

In this context, we recently discovered a large density of bipolarons near the anode interface between indium-tin oxide (ITO) and the common hole transport material *N,N'*-bis(3-methylphenyl)-*N,N'*-diphenylbenzidine (TPD) [3]. On the basis of interface energy level modeling, we concluded that bipolaron formation is generally favorable near electrodes because the interface energetic disorder often exceeds that in the bulk and because the contact can pin the Fermi level deep in the resulting density of states distribution. A third reason, however, which was not discussed in the work above, is that the bipolaron is electrostatically stabilized by its image charge in the electrode to a greater degree than two individual polarons. This basic effect was noted early on by Saxena and co-workers [4,5] in the context of previous work on bipolaron formation at metal-polymer interfaces [6–9]; however, its

impact in the case of small molecule organic semiconductors with significant energetic disorder has yet to be explored.

Here, we revisit the image charge stabilization of bipolarons with a simple electrostatic model that we validate for TPD with density functional theory (DFT) calculations. Incorporating this effect into our interface energetic model, we find that it strongly enhances bipolaron formation in the first one to two monolayers and leads to the expectation that bipolarons constitute $> 1\%$ of the total interfacial charge density over a broad range of realistic model parameters. These results reinforce the notion that bipolaron formation is a robust interfacial phenomenon in organic semiconductor devices and motivate experiments to understand how it affects current injection in the context of unipolar organic magnetoresistance.

II. THEORY

The enhancement in bipolaron stability that occurs near a conducting interface can be understood from a simple point charge approximation of two nearby TPD polarons and their image charges illustrated in Fig. 1(a). In addition to the usual Coulomb interaction for each charge with its own image (U_{direct} which leads to, e.g., Schottky barrier lowering for individual holes and electrons) [10], it is also stabilized by the image of its neighbor (U_{cross} , dashed green arrows in Fig. 1). In the limit that the charges move together and form a point bipolaron with charge $2q$, the direct and cross term interactions are equal ($U_{\text{direct}} = U_{\text{cross}}$), leading to a bipolaron stabilization of $4U_{\text{direct}} \propto (2q)^2$ that is twice that of two infinitely separated polarons, $2U_{\text{direct}} \propto q^2 + q^2$. Figure 1(b) plots the change in total electrostatic energy of each case from its “bulk” reference value at a distance $z = 5$ nm from the interface (dotted lines), demonstrating that a bipolaron becomes increasingly

*ncg2@psu.edu

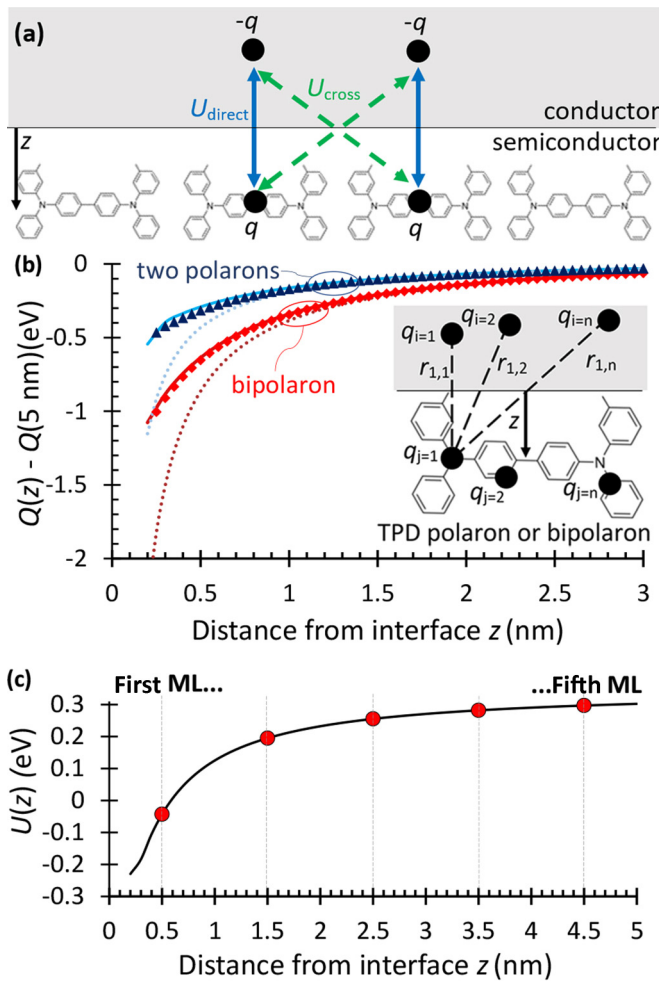


FIG. 1. (a) Point charge representation of two nearby polarons at an organic semiconductor/electrode interface. In addition to interacting with its own image charge (U_{direct}), each polaron increasingly interacts with the image of its neighbor (U_{cross}) as the polarons move closer to form a bipolaron. (b) Change in energy of a bipolaron (red) and two polarons (blue, infinite lateral spacing) as they approach a conducting interface, relative to their energies in the bulk at $z = 5$ nm. Approximating each species as a single point charge (dashed lines) maintains good agreement with density functional theory (DFT) calculations carried out for the molecule TPD except for distances within ~ 1 nm of the interface. The accuracy in this near-surface region can be improved (solid lines) by dividing the full charge of a TPD polaron or bipolaron into $n = 72$ fractional charges and their images (q_j and q_i , respectively) associated with each atomic coordinate of the molecule as depicted in the inset (only three charges are drawn for simplicity). (c) Results of Eq. (2) in the text showing how the Hubbard energy for formation of a TPD bipolaron decreases from its bulk value of $U_0 = 0.35$ eV as it approaches an electrode interface. The red circles highlight the values of $U(z)$ in the middle of each TPD monolayer (ML, the center of which is denoted by the dashed lines) assumed in the model results presented in Figs. 2 and 3.

stable relative to two polarons as they get closer to the interface.

Density functional theory calculations confirm this stabilization enhancement in Fig. 1(b) (symbols), but indicate that the

point charge approximation breaks down within ~ 1 nm of the interface. The calculations are carried out using the B3LYP functional with a 6-31G** split valence plus polarization basis set (B3LYP/6-31g**) for an isolated molecule assuming a background relative dielectric constant, $\epsilon_r = 3$. The tacit assumption that polarons and bipolarons are localized on individual molecules follows from the fact that their optical absorption spectra in a thin film are nearly identical to that of isolated cations and dications in solution [3]. The metal is accounted for by including the mirror image of the molecular charge distribution as an external electrostatic contribution to the DFT potential when computing different charge and spin states of TPD. Although many bipolaron orientations are nominally possible in a disordered organic semiconductor, we limit our focus here to TPD bipolarons that are parallel to the interface because this configuration leads to the greatest stabilization (and thus is most likely to be formed in practice) and because molecules similar to TPD often lie flat in the first few monolayers when deposited on a high work function conducting substrate [11]. It is also worth noting that the DFT stabilization behavior in Fig. 1 is virtually unaffected by differences in bipolaron spin state or molecular conformation, as all three forms of the bipolaron (i.e., the singlet and triplet states as well as the diradical with holes located on opposite arylamine fragments due to a dihedral twist in the central biphenyl moiety [3]) exhibit a nearly identical energy reduction relative to their $z = 5$ nm references in the bulk (which do differ in energy).

The short-range accuracy of the point charge model can be improved by splitting the charge of a polaron or bipolaron into n fractional elementary charges (q_j) and placing them at each atomic coordinate (x, y, z) in accord with the DFT charge distribution. An image charge configuration is then created with oppositely signed fractional charges (q_i) located at ($x, y, -z$) and the electrostatic energy of the system is calculated via

$$Q(z) = U_Q + \frac{1}{2} \sum_{i=1}^n \sum_{j=1}^n \frac{q_j q_i}{4\pi \epsilon_0 \epsilon_r r_{j,i}}, \quad (1)$$

where ϵ_0 is the permittivity of free space, $r_{j,i}$ is the distance between the real and image charges, and the sums run over the $n = 72$ atoms that make up TPD. The factor of $\frac{1}{2}$ is included because the electric field distribution in the conductor is fictitious and does not actually store any energy [10]. The electrostatic energy associated with the partial charge distribution of the molecule itself is represented by U_Q , and is assumed to be independent of z since the DFT results do not show any appreciable reorganization of the nuclear framework or redistribution among the partial charges as the polaron/bipolaron moves closer to the interface. Evaluating the image stabilization of the polaron and bipolaron with Eq. (1) subsequently leads to much better agreement with the DFT data as shown by the solid lines in Fig. 1(b). This is important because it means that, short of chemisorptive interactions (e.g., formation of new hybrid orbitals at the interface), Eq. (1) provides an efficient way of extrapolating the DFT energy of a polaron or bipolaron in the bulk to nearly any distance from an electrode interface.

Given that the nuclear reorganization of both the polaron and bipolaron are essentially unaffected by their electrostatic interaction with the conductor, the Hubbard energy required to form a bipolaron from two polarons near the electrode, $U(z)$, should be the same as in the bulk (U_0) except for the electrostatic energy difference between the two charge configurations:

$$U(z) = U_0 + \frac{1}{2} \sum_{i=1}^n \sum_{j=1}^n \frac{q_j q_i}{4\pi \epsilon_0 \epsilon_r r_{j,i}} - \frac{1}{2} \sum_{i=1}^{2n} \sum_{j=1}^{2n} \frac{q_j q_i}{4\pi \epsilon_0 \epsilon_r r_{j,i}}, \quad (2)$$

where the middle term sums over the n partial charges of the bipolaron and the last term sums over the $2n$ partial charges of two polarons (which may or may not be close enough for mutual image charge interaction). Taking $U_0 = 0.35$ eV for TPD [3] and two infinitely spaced polarons as the reference point in Eq. (2), Figure 1(c) shows that bipolaron formation becomes barrierless in the first monolayer at $z \approx 0.5$ nm.

To understand how this image charge stabilization impacts the bipolaron density at a realistic TPD/electrode interface, we adopt the interface energetic model formulated for polarons by

Oehzelt *et al.* [12] and subsequently extended to bipolarons by Dhanker *et al.* [3]. In this case, however, we modify the Hubbard energy from Ref. [3] to include the z -dependent image stabilization from the electrode described by Eq. (2). Briefly, this model iteratively determines the polaron and bipolaron density within an energetically disordered density of states (DOS) distribution near a conducting interface by solving Poisson's equation in one dimension under the constraint that the Fermi level (E_F) set by the electrode work function (φ_A) remains flat throughout the system. In the case at hand, we focus on the highest occupied molecular orbital (HOMO) DOS of TPD and approximate it as a Gaussian:

$$g(E) = \frac{N_{\text{mol}}}{\sqrt{2\pi}\sigma^2} \exp(-[E - E_H + qV(z)]^2/2\sigma^2), \quad (3)$$

characterized by the HOMO energy E_H , the density of molecular sites N_{mol} , the potential difference between the electrode interface and the center of the layer $V(z)$, and the DOS width σ . The probability that a given state in $g(E)$ is occupied by a hole polaron [$f_p(E)$] or bipolaron [$f_{bp}(E)$] is given by their respective Fermi occupation functions [8,13]:

$$f_p(E) = \frac{2\exp[(E - E_F)/kT]}{1 + 2\exp[(E - E_F)/kT] + \exp([2(E - E_F) - U(z)]/kT)}, \quad (4)$$

$$f_{bp}(E) = \frac{\exp([2(E - E_F) - U(z)]/kT)}{1 + 2\exp[(E - E_F)/kT] + \exp([2(E - E_F) - U(z)]/kT)}, \quad (5)$$

with the empty state probability equal to $1 - f_p - f_{bp}$. The total charge density is thus

$$\rho(z) = qN_{\text{mol}} \int f_p(E)g(E)dE + 2qN_{\text{mol}} \int f_{bp}(E)g(E)dE. \quad (6)$$

Note that the description of polaron and bipolaron occupation given by Eqs. (4)–(6) is different than we previously used in Ref. [3]. Both approaches yield similar results over a wide range of input parameters; however, the description used here maintains a more physically realistic description when the Hubbard energy becomes negative, which can occur close to the interface per Fig. 1(b).

The potential, $V(z)$, is determined by solving the Poisson equation discretely in one dimension using the method of images (which naturally imposes the boundary condition $V(0) = 0$ at the conductor surface and the requirement that $dV/dx \rightarrow 0$ in the bulk of the film [10]) assuming sheet charge densities, ρ_k , located at the center of each $d = 1$ nm-thick monolayer [12]. Image sheet charges ($-\rho_k$) are reflected on the other side of the metal interface for all m layers of organic material and the potential difference between the interface and the center of each monolayer is calculated from Gauss's law:

$$V(z) = \sum_{k=1}^m \frac{\rho_k d}{\epsilon_r \epsilon_0} z_{\text{min}}, \quad (7)$$

where z_{min} is either the distance from the interface to the center of layer k , or z , whichever is smaller for each layer k .

The solution procedure is iterative and begins by guessing ρ_k for each layer, using that to compute $V(z)$ as described by Eq. (7), and then using $V(z)$ to calculate ρ_k using Eq. (6). Each value of ρ_k is adjusted until it is self-consistent with the result of Eq. (6) for all layers. For example, solving Eq. (6) for a 5-nm-thick organic film with $d = 1$ nm means solving five transcendental equations, with five values of $U(z)$ for input as highlighted by the red circles in Fig. 1(c). The polaron density $P^+ = \int f_p(E)g(E)dE$, and bipolaron density $P^{2+} = \int f_{bp}(E)g(E)dE$ are subsequently evaluated in each layer using Eq. (6), which allows the bipolaron fraction of charged molecules, $\beta_{BP} \equiv P^{2+}/(P^+ + P^{2+})$, to be determined throughout the film.

III. RESULTS

Figure 2 shows the result of this model for the interface between ITO and TPD examined in Ref. [3] based on the following parameters: $\varphi_A = 5.1$ eV, $E_H = 5.3$ eV, $\sigma = 0.1$ eV, $U_0 = 0.35$ eV, $N_{\text{mol}} = 10^{21}$ cm $^{-3}$, and $\epsilon_r = 3$, with an ambient temperature, $T = 298$ K. For the sake of clarity, we do not assume enhanced disorder in the first monolayer as we did in Ref. [3] because it obscures the image stabilization effect being studied here; including this added interfacial broadening would simply favor bipolaron formation even further in the results below. According to Fig. 2(a), the image stabilization effect dramatically increases bipolaron formation in the first several monolayers, boosting β_{BP} from a negligible

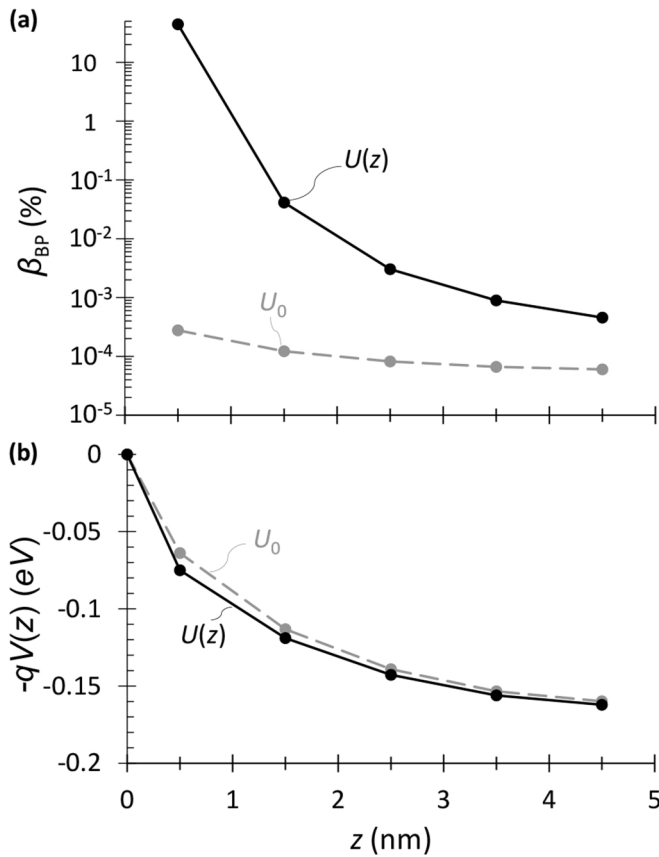


FIG. 2. (a) Bipolaron fraction of charged species (β_{BP}) calculated as a function of distance from the interface (z) when including $[U(z)]$, and neglecting (U_0), the enhanced stabilization of bipolarons caused by the image charge effect. Bipolaron formation is most significant near the interface due to the strong image charge stabilization shown graphically in Fig. 1(c). (b) Inclusion of the image effect does not significantly change the potential distribution or net charge density in the organic material; it mainly affects the balance of charge that exists in the form of polarons versus bipolarons as shown in (a). In this calculation, we assume $\varphi_A = 5.1$ eV, $E_H = 5.3$ eV, $\sigma = 0.1$ eV, $U_0 = 0.35$ eV, $N_{mol} = 10^{21}$ cm $^{-3}$, $\epsilon_r = 3$, and an ambient temperature, $T = 298$ K as described in the text.

value in the case of no image effect to $\sim 40\%$ at $z = 0.5$ nm. As expected, β_{BP} falls off quickly upon moving away from the interface due to the rapid increase of $U(z)$ illustrated in Fig. 1(c). It is important to emphasize, however, that the total charge transferred, and thus the potential shift $V(z)$ shown in Fig. 2(b), is largely the same in both cases; the inclusion of $U(z)$ mainly just affects the balance between polaron and bipolaron states.

Figures 3(a)–3(d) summarize the impact of the key parameters in the model where, in all cases, including the image charge stabilization in the Hubbard energy via Eq. (2) substantially increases the total bipolaron fraction in the film (i.e., β_{BP} calculated from the integrals of P^+ and P^{2+} over the film thickness). In Fig. 3(a), more bipolarons form with increasing energetic disorder as discussed in Ref. [3]. Increasing the bulk Hubbard energy U_0 in Fig. 3(b) obviously inhibits bipolaron formation. Similarly, the bipolaron density increases with increasing electrode work function in Fig. 3(c)

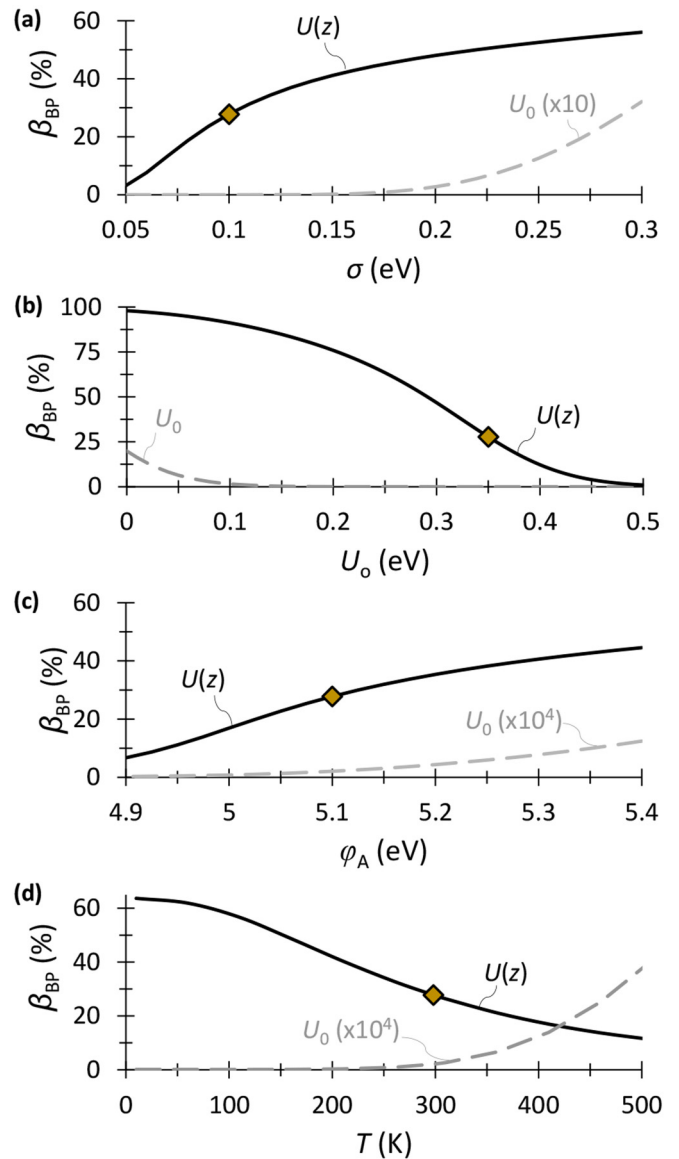


FIG. 3. Bipolaron fraction of charged species in the entire organic film (β_{BP} calculated from the integral of polaron and bipolaron densities) when including $[U(z)]$ and neglecting (U_0) the bipolaron image stabilization effect. (a) Increasing the HOMO DOS width (σ) increases β_{BP} in both cases. (b) Increasing the bulk formation energy decreases β_{BP} , though it remains greater than 1% for $U_0 > 0.5$ eV when the image effect is accounted for. (c) The bipolaron fraction increases as the anode work function (φ_A) shifts the Fermi level deeper into the HOMO DOS. (d) As discussed in the text, increasing temperature is predicted to increase β_{BP} for the constant U_0 case but to decrease β_{BP} when the image stabilization is accounted for. The gold diamonds in each plot denote the particular case shown in Fig. 2. Numbers beside U_0 in parentheses indicate the factor β_{BP} is scaled by for visibility on the plot. All of the results above are calculated for a 5-nm-thick TPD layer using the model described in the text with the following parameters unless otherwise stated: $U_0 = 0.35$ eV, $E_H = 5.3$ eV, $\varphi_A = 5.1$ eV, $\sigma = 0.1$ eV, $\epsilon_r = 3$, and $T = 298$ K.

as E_F is pinned deeper in the HOMO DOS. Interestingly, increasing temperature is predicted to increase β_{BP} for the constant Hubbard energy (U_0) case but to decrease β_{BP} when the image stabilization is accounted for. When the barrier

to bipolaron formation is large, as it is in the constant U_0 case, $f_{bp}(E)$ and $f_p(E)$ both broaden with increasing temperature, but the overlap between $f_{bp}(E)$ and the rapidly varying DOS tail increases faster than that between $f_p(E)$ and the slowly varying DOS bulk, hence β_{BP} increases. Conversely, when the barrier for bipolaron formation is small (as in the first monolayer of the image-stabilized case), both occupation functions compete for the same portion of the DOS, causing $f_p(E)$ to displace some of the bipolaron states as it broadens, reducing β_{BP} . For the parameters used here, this transition in the temperature dependence occurs when the local Hubbard energy is approximately 0.15 eV.

We note that there is an additional complication that arises at high charge density since polarons may get close enough to each other to experience some mutual image stabilization reflected in the last term of Eq. (2), thus effectively causing $U(z)$ to depend on $\rho(z)$. Moreover, when two polarons form a bipolaron, the total number of occupied sites is reduced, allowing for the charges to spread out more and achieve a lower total energy in equilibrium. We find, however, that both effects are negligible when the total fraction of occupied sites is less than $\sim 10\%$ (which is the case for all of the parameter variations considered in Fig. 3) and thus they are not expected to be important in most cases of practical interest.

IV. DISCUSSION

Taken together, the results from Fig. 3 demonstrate that the image enhancement in bipolaron stability enables β_{BP} to become non-negligible (i.e., $>1\%$) over a broad range of realistic input parameters. This is significant because in our previous work [3], we had to invoke an unusually high disorder width ($\sigma > 0.2$ eV) and low Hubbard energy ($U_0 = 0.25$ eV) to explain the experimentally observed $\beta_{BP} \sim 1\%$. When the image stabilization effect is taken into account, bipolaron fractions of this magnitude can be explained more naturally. Given the role of bipolarons in organic magnetoresistance [2], the image effect may also help explain the large change in magnetoresistance that is observed upon adding a self-assembled monolayer to the anode contact of TPD-based diodes [14], since spacing bipolarons farther from the anode would reduce their image stabilization per Fig. 1(c).

It would be interesting in the future to compare the results of this model to a kinetic Monte Carlo approach where all Coulomb interactions can be explicitly accounted for in three dimensions and under nonequilibrium conditions (i.e., under

bias). In addition to providing a more accurate description of the electrostatic environment and incorporating the kinetics of bipolaron formation/dissociation, this approach would enable the relative impact of magnetic field-dependent injection to be explored in analogous fashion to previous work focused on the bulk [2,13,15].

If bipolaron-mediated magnetoresistance is indeed an interface rather than a bulk effect, then it motivates device design strategies for enhancement, such as increasing the electrode surface roughness on both the molecular scale (which increases image stabilization on average [16,17]) and the mesoscale (which increases the amount of magnetoactive electrode interface per unit device area). Alternatively, bipolarons could be stabilized in the channel of field effect transistors [18] by their image in the gate electrode, potentially enabling a larger magnetoresistance effect than injection through a thin interfacial layer in sandwich-type devices. While Fig. 1(c) suggests that an unrealistically thin (~ 1 nm) gate dielectric would be needed to achieve appreciable stabilization, we note that the effect is not limited to virtual image charges, but can also result from real counterions [4] and thus a similar stability enhancement might manifest in electric double-layer gated transistors where electrolyte counterions accumulate within ~ 1 nm of the organic semiconductor surface [19].

V. CONCLUSION

We find that the image charge interaction that arises from explicitly considering the spatial extent of a bipolaron near a conducting interface stabilizes this species by up to ~ 0.3 eV for a prototypical molecule such as TPD. Accounting for this effect in an equilibrium model of the interfacial charge density dramatically increases the bipolaron concentration in the first few monolayers, typically exceeding 1% of the total charge density for a broad range of realistic material parameters. This finding is important because it addresses what is arguably the biggest objection to the bipolaron model of organic magnetoresistance—that the Hubbard energy is simply too high for bipolarons to form—and thus motivates renewed experimental effort to probe the role of injection in organic magnetoresistance.

ACKNOWLEDGMENTS

This work was supported in part by the U.S. Department of Energy, Office of Basic Energy Sciences under Award No. DE-SC0012365.

-
- [1] A. Kohler and H. Bassler, *Electronic Processes in Organic Semiconductors* (Wiley-VCH, Berlin, 2015), pp. 161–165.
 - [2] P. A. Bobbert, T. D. Nguyen, F. W. A. van Oost, B. Koopmans, and M. Wohlgenannt, Bipolaron Mechanism for Organic Magnetoresistance, *Phys. Rev. Lett.* **99**, 216801 (2007).
 - [3] R. Dhankar, C. Gray, S. Mukhopadhyay, S. Nunez, C. Cheng, A. Sokolov, and N. C. Gebink, Large bipolaron density at organic semiconductor/electrode interfaces, *Nat. Commun.* **8**, 2252 (2017).
 - [4] S. Brazovskii, N. Kirova, Z. G. Yu, A. R. Bishop, and A. Saxena, Stability of bipolarons in conjugated polymers, *Opt. Mater.* **9**, 502 (1998).
 - [5] A. Saxena, S. Brazovskii, N. Kirova, Z. G. Yu, and A. R. Bishop, Stability of bipolarons in conjugated polymers, *Synth. Met.* **101**, 325 (1999).
 - [6] S. A. Brazovskii and N. N. Kirova, Towards the theory of metal-polymer contact, *Synth. Met.* **57**, 4385 (1993).
 - [7] N. Kirova and M.-N. Bussac, Self-trapping of electrons at the field-effect junction of a molecular crystal, *Phys. Rev. B* **68**, 235312 (2003).

- [8] P. S. Davids, A. Saxena, and D. L. Smith, Nondegenerate continuum model for polymer light-emitting diodes, *J. Appl. Phys.* **78**, 4244 (1995).
- [9] P. S. Davids, A. Saxena, and D. L. Smith, Bipolaron lattice formation at metal-polymer interfaces, *Phys. Rev. B* **53**, 4823 (1996).
- [10] D. J. Griffiths, *Introduction to Electrodynamics*, 4th ed. (Addison-Wesley, Boston, 2012).
- [11] T. Matsushima and H. Murata, Charge transfer-induced horizontal orientation of organic molecules near transition metal oxide surfaces, *Org. Electron.* **14**, 1149 (2013).
- [12] M. Oehzelt, N. Koch, and G. Heimel, Organic semiconductor density of states controls the energy level alignment at electrode interfaces, *Nat. Commun.* **5**, 4174 (2014).
- [13] N. Gao, L. Li, N. Lu, C. Xie, M. Liu, and H. Bassler, Unified percolation model for bipolaron-assisted organic magnetoresistance, *Phys. Rev. B* **94**, 075201 (2016).
- [14] H. Jang, S. J. Pookpanratana, A. N. Bridgeman, R. J. Kline, J. I. Basham, D. J. Gundlach, C. A. Hacker, O. A. Kirillov, O. D. Jurchescu, and C. A. Richter, Interface engineering to control magnetic field effects of organic based devices by using a molecular self-assembled monolayer, *ACS Nano* **8**, 7192 (2014).
- [15] W. Wagemans, F. L. Bloom, P. A. Bobbert, M. Wohlgenannt, and B. Koopmans, A two-site bipolaron model for organic magnetoresistance, *J. Appl. Phys.* **103**, 07F303 (2008).
- [16] G. Palasantzas, Roughness effects on the electrostatic-image potential near a dielectric interface, *J. Appl. Phys.* **82**, 351 (1997).
- [17] T. S. Rahman and A. A. Maradudin, Effect of surface roughness on the image potential, *Phys. Rev. B* **21**, 504 (1980).
- [18] C. Isenberg and T. P. I. Saragi, Revealing the origin of magnetoresistance in unipolar amorphous organic field-effect transistors, *J. Mater. Chem. C* **2**, 8569 (2014).
- [19] S. H. Kim, K. Hong, W. Xie, K. H. Lee, S. Zhang, T. P. Lodge, and C. D. Frisbie, Electrolyte-gated transistors for organic and printed electronics, *Adv. Mater.* **25**, 1822 (2013).